Scattering Function of Isotactic Oligo- and Poly(methyl methacrylate)s in Dilute Solution

Ken Horita,† Takenao Yoshizaki,† Hisao Hayashi,‡ and Hiromi Yamakawa*,†

Department of Polymer Chemistry, Kyoto University, Kyoto 606-01, Japan, and Department of Materials Chemistry, Faculty of Science and Technology, Ryukoku University, Seta, Otsu 520-21, Japan

Received July 5, 1994®

ABSTRACT: The scattering function was determined for four samples of isotactic oligo- and poly(methyl methacrylate)s (i-PMMA), each with the fraction of racemic diads $f_r \simeq 0.01$, in the range of weight-average molecular weight M_w from 1.01×10^3 to 9.87×10^4 in acetonitrile at 28.0 °C (Θ) for the magnitude k of the scattering vector smaller than 1 Å^{-1} by the use of a point-focusing small-angle X-ray scattering (SAXS) camera. The Kratky function F_s as a function of k increases monotonically with increasing k irrespective of the values of M_w and does not exhibit a maximum followed by a minimum, as observed for atactic (a-) or syndiotactic (s-) PMMA. It is shown that the helical wormlike (HW) chain theory may explain rather well the present SAXS data over the whole range of k studied. However, the agreement between theory and experiment in the range of large k may be only accidental. A rather detailed comparison is made of the present data for i-PMMA with the previous data for a-PMMA with $f_r = 0.79$ and s-PMMA with $f_r = 0.92$ in acetonitrile at 44.0 °C (Θ), and the dependence of F_s on f_r is discussed, it being consistent with the HW theory. A comparison is also made of the present SAXS data with literature data obtained for i-PMMA in the bulk from small-angle neutron scattering (SANS) measurements. As in the case of a-PMMA, it is concluded that the difference between the Kratky plots (F_s) of the two kinds of data in the range of large k arises from the difference in the distribution of scatterers between SAXS and SANS.

Introduction

In a previous paper,[1] we studied the mean-square radius of gyration $\langle S^2 \rangle$ of isotactic poly(methyl methacrylate) (i-PMMA) with the fraction of racemic diads $f_r \simeq 0.01$ in the unperturbed Θ state over a wide range of molecular weight M, including the oligomers with very low M. The results obtained there for i-PMMA have been compared with the previous ones for atactic (a-) PMMA with $f_r = 0.79$,[2] and from an analysis of the M dependence of $\langle S^2 \rangle / M$ on the basis of the helical wormlike (HW) chain,[3,4] it has then been shown that the former chain is of weaker helical nature than the latter, which retains rather large and clearly distinguishable helical portions in dilute solution. It must however be noted that, although the helical nature of the i-PMMA chain is not very strong, the dependence of its $\langle S^2 \rangle / M$ on M can be explained neither by the Kratky–Porod wormlike chain[5] nor by the Gaussian chain model. Such a difference in local chain conformation may be considered to be more sensitively reflected in the behavior of the scattering function determined by small-angle X-ray scattering (SAXS). Thus, in the present study, we do this for i-PMMA and compare the results with the previous ones for a-PMMA[6] and also for syndiotactic (s-) PMMA with $f_r = 0.92$.[7]

Thirty years ago, similar experimental studies were carried out by Kirste and Wunderlich[8,9] in the same spirit. As noted in the previous papers,[6,7] however, their SAXS results for a- and s-PMMAs seem to be quite doubtful, especially in the range of the large magnitude k ($\gtrsim 0.4$ Å^{-1}) of the scattering vector. The shortcomings of their data may be regarded as arising from the fact that the use of the Kratky SAXS camera with the data processing (desmearing) procedure inherent in it loses the reliability of the data in such a range of large k. As claimed in the previous papers,[6,7] on the other hand, our SAXS data were taken by the use of a point-focusing SAXS camera, with which the scattering function may be directly determined without any data processing. Thus, also for the present purpose, it is necessary and interesting to determine unambiguously the scattering function by the use of the same point-focusing camera as used in the previous studies.[6,7]

The present SAXS measurements on i-PMMA were carried out in acetonitrile at the Θ temperature 28.0 °C determined previously.[1] It had also been used as a common Θ solvent for a- and s-PMMAs (with Θ = 44.0 °C[2,7]) in the previous SAXS measurements.[6,7] Thus the SAXS data for the three kinds of PMMA in the same solvent may be directly compared.

Experimental Section

Materials. Three of the four i-PMMA samples used, iOM10, iOM31, and iMM1, are the same as those used in the previous study[1] of $\langle S^2 \rangle$, i.e., the fractions separated by gel permeation chromatography and/or fractional precipitation from the original whole samples prepared by living anionic polymerization, following the procedure of Ute et al.[10] The remaining one, iMMc10, is the same as that used in a study of transport coefficients,[11] i.e., a fraction separated from a commercial sample 9011-14-7 of Scientific Polymer Products, Inc. The values of f_r for these samples are ca. 0.01, independent of the weight-average molecular weight M_w. The values of M_w determined from light scattering (LS) measurements,[1,11] the weight-average degree of polymerization x_w, the ratio of M_w to the number-average molecular weight M_n, and the root-mean-square radius of gyration $\langle S^2 \rangle^{1/2}$ determined from SAXS in acetonitrile at 28.0 °C (Θ)[1] are summarized in Table 1.

The solvent acetonitrile used for SAXS measurements was purified according to a standard procedure.

Small-Angle X-ray Scattering. As in the previous SAXS studies,[6,7,12] all measurements were carried out by the use of a point-focusing camera of overall length 6 m in the High-Intensity X-ray Laboratory of Kyoto University. A detailed specification of this camera has already been given elsewhere[13] and its brief description has been given in the previous paper.[12] Thus we here note only a few points appropriate to the present work.

* To whom all correspondence should be addressed.
† Kyoto University.
‡ Ryukoku University.
® Abstract published in *Advance ACS Abstracts*, September 15, 1994.

0024-9297/94/2227-6492$04.50/0

Table 1. Values of M_w, x_w, M_w/M_n, and $\langle S^2\rangle^{1/2}$ for Isotactic Oligo- and Poly(methyl methacrylate)s

sample	M_w	x_w	M_w/M_n	$\langle S^2\rangle^{1/2}$, Å
iOM10[a]	1.01×10^3	9.52	1.02	7.5_9
iOM31	3.12×10^3	30.6	1.04	$15._6$
iMM1	1.07×10^4	106	1.05	$29._9$
iMMc10	9.87×10^4	986	1.08	

[a] All values of M_w had been determined from LS in acetonitrile at 28.0 °C,[1,11] and all values of $\langle S^2\rangle^{1/2}$ from SAXS also in acetonitrile at 28.0 °C.[1]

In this work, the Mo Kα line of wavelength $\lambda_0 = 0.711$ Å was used as the incident beam by eliminating other lines with a Zr foil of 50-μm thickness. The distance from a sample cell to a detector (two-dimensional position-sensitive proportional counter) was ca. 640 mm, as before,[6,7,12] so that intensity measurements could be carried out in the range of k up to ca. 1 Å^{-1}. The temperature of the sample cell was kept constant at 28.0 ± 0.1 °C for the acetonitrile solutions. The excess scattering intensity in the range $k \gtrsim 0.5$ Å^{-1} was very small. Therefore, in order to diminish statistical errors in this range, the intensities scattered from each solution and the solvent were accumulated for ca. 12 and 6 h, respectively. The measurements on the solvent were made before and after every measurement on the solution.

As in the previous studies,[6,7,12] the two-dimensional data thus obtained for a solution of solute mass concentration c (in g/cm^3) were first corrected for the detector sensitivity and then averaged over polar angles in the detector plane to obtain the scattering intensity $I_{obs}(k,c)$ as a function of k, which is explicitly defined by

$$k = (4\pi/\lambda_0)\sin(\theta/2) \tag{1}$$

with θ the scattering angle. From the observed intensity I_{obs}, we evaluate the reduced intensity $I_R(k,c)$ defined by

$$I_R(k,c) = I_{obs}(k,c)/AI_0 \tag{2}$$

where A is the transmittance of a given sample solution and I_0 is the intensity of the incident beam monitored by the intensity scattered from a polyethylene film placed in front of the detector. The excess reduced scattering intensity $\Delta I_R(k,c)$ is then obtained as the reduced scattering intensity from the solution $I_{R,soln}(k,c)$ minus that from the solvent $I_{R,solv}(k)$ [$=I_{R,soln}(k,0)$] as follows:

$$\Delta I_R(k,c) = I_{R,soln}(k,c) - I_{R,solv}(k) \tag{3}$$

Results

Following the same procedure as used in the previous studies of the scattering function,[6,12] we first evaluate the (normalized) scattering function P_s from the values of the excess reduced scattering intensity $\Delta I_R(k,c)$, which are directly obtained from SAXS measurements, as mentioned in the Experimental Section.

It may be summarized as follows. The quantity $\Delta I_R(k,c)$ may be written in terms of P_s as[6,12]

$$\frac{Kc}{\Delta I_R(k,c)} = \frac{1}{M_w P_s(k)} + 2A_2Q(k)c + \mathcal{O}(c^2) \tag{4}$$

where K is the optical constant, A_2 is the second virial coefficient, and Q represents the intermolecular interference.[14] (Note that P_s and Q become unity at $k = 0$.) From eq 4, we obtain

$$\frac{\Delta I_R(k,c)}{KM_wc} = P_s(k) - 2A_2M_w[P_s(k)]^2Q(k)c + \mathcal{O}(c^2) \tag{5}$$

We may then evaluate P_s by extrapolating the ratio $\Delta I_R(k,c)/KM_wc$ to $c = 0$ if the value of K is known. In the limits of $k \to 0$ and $c \to 0$, we have from eq 4

$$K = [\Delta I_R(0,c)/c]_{c=0}/M_w \tag{6}$$

Thus K may be evaluated experimentally if the value of $[\Delta I_R(0,c)/c]_{c=0}$ is determined for a sample whose M_w is known.

In the present case, we evaluated $[\Delta I_R(0,c)/c]_{c=0}$ for the sample iOM31 in acetonitrile at 28.0 °C by the use of the Berry square-root plot.[15] For each solution of this sample, the plot of $(c/\Delta I_R)^{1/2}$ against k^2 followed a straight line in the range of small k, so that the intercept $[c/\Delta I_R(0,c)]^{1/2}$ at a given c could be unambiguously determined. Similarly, in the range of small k, the plot of $(c/\Delta I_R)^{1/2}$ against c was fitted by a straight line and could be extrapolated to infinite dilution to evaluate $[c/\Delta I_R(k,c)]^{1/2}_{c=0}$ at a given (small) k. The values of $[c/\Delta I_R(0,c)]^{1/2}$ and $[c/\Delta I_R(k,c)]^{1/2}_{c=0}$ thus determined for the sample iOM31 are plotted against c and k^2, respectively, in Figure 1. The two kinds of plots can be extrapolated to obtain the common intercept $[c/\Delta I_R(0,c)]^{1/2}_{c=0} = 38.1$ (g/cm^3)$^{1/2}$. With the value of M_w for the sample iOM31 given in Table 1, K is thus evaluated to be 2.21×10^{-7} cm^3/g.

Before presenting results for the scattering function, it is interesting here to compare the value of the apparent mean-square radius of gyration $\langle S^2\rangle_s$, which may be evaluated from the data presented in Figure 1, with that determined in the previous study[1] of $\langle S^2\rangle$. Note that $\langle S^2\rangle_s$ is defined in the equation

$$P_s(k) = 1 - (1/3)\langle S^2\rangle_s k^2 + \mathcal{O}(k^4) \tag{7}$$

It may then be determined from the intercept and initial slope of the plot of $[c/\Delta I_R(k,c)]^{1/2}_{c=0}$ against k^2 in Figure 1. The result thus obtained for $\langle S^2\rangle_s$ is 242 Å^2. This value is in rather good agreement with the corresponding value 253 Å^2 determined previously,[1] indicating that the present determination of the scattering intensity is consistent with the previous one with a Kratky camera in the range of small k. (Note that $\langle S^2\rangle_s$ should in general be distinguished from the mean-square radius of gyration $\langle S^2\rangle$ of the chain contour except for long enough chains.[1])

Now, Figure 2 shows plots of $k^2\Delta I_R(k,c)/Kc$ against k for the sample iOM31 in acetonitrile at various c at 28.0 °C. The ordinate quantity corresponds to the (absolute-scale) Kratky function $F_s(k)$ defined by

$$F_s(k) = M_w k^2 P_s(k) \tag{8}$$

(at finite concentrations), the above plot being just the Kratky plot. In the figure, the unfilled, right-half-filled, and left-half-filled circles represent the values at $c = 0.0814$, 0.0571, and 0.0444 g/cm^3, respectively. We note that the scattering data for the sample iOM31 at the lowest concentration ($c = 0.0269$ g/cm^3) are less accurate than those at higher concentrations in the range $k \gtrsim 0.5$ Å^{-1} because of the weakness of the excess scattering intensity, and therefore those data points have been omitted in the figure. It is seen that the plot is almost independent of c in the range of k displayed, as in the case of a- and s-PMMAs,[6,7] so that we adopt as before[6,7] the values of $\Delta I_R(k,c)/KM_wc$ at the highest concentration as those of the scattering function P_s for the single polymer chain at infinite dilution. We note that, in the range of small k, the concentration dependence is appreciable in the plot displayed in Figure 1 but cannot be recognized in the Kratky plot and also that, for atactic polystyrene (a-PS) in cyclohexane at 34.5 °C (Θ), the Kratky plot depends appreciably on c in the range $k \gtrsim 0.1$ Å^{-1}, in contrast to the case of PMMAs including i-PMMA.

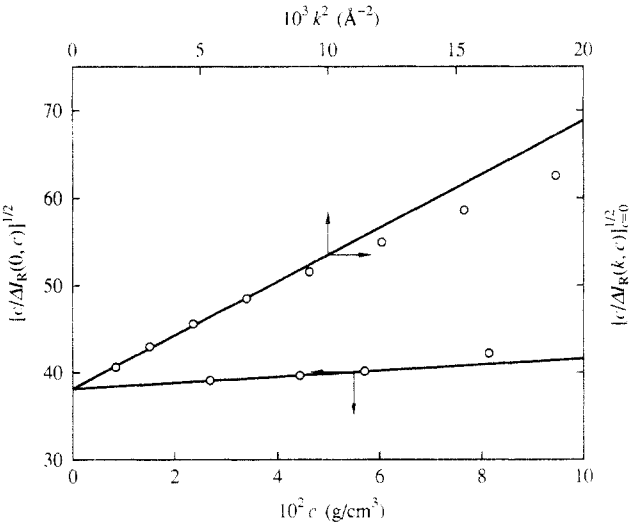

Figure 1. Plots of $[c/\Delta I_R(0,c)]^{1/2}$ and $[c/\Delta I_R(k,c)]^{1/2}_{c=0}$ against c and k^2, respectively, for sample iOM31 in acetonitrile at 28.0 °C.

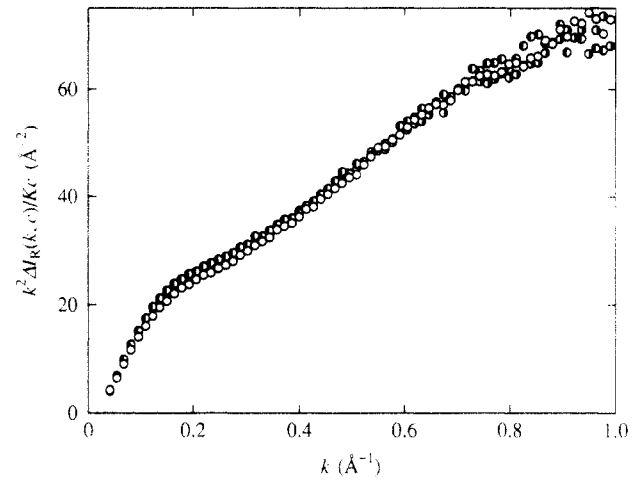

Figure 2. Plots of $k^2\Delta I_R(k,c)/Kc$ against k for sample iOM31 in acetonitrile at 28.0 °C: (○) c = 0.0814 g/cm^3; (◑) c = 0.0571 g/cm^3; (◐) c = 0.0444 g/cm^3.

Figure 3 shows plots of $F_s(k)$ against k for all the i-PMMA samples in acetonitrile at 28.0 °C, where the data points for the samples iOM31, iMM1, and iMMc10 have been shifted upward by 20, 40, and 60 Å^{-2}, respectively, for convenience. $F_s(k)$ increases monotonically with increasing k for each sample and does not exhibit a maximum followed by a minimum, as observed for a- and s-PMMAs[6,7] with $M_w \gtrsim 10^4$. The scattering profile for i-PMMA for $k \lesssim 0.3$ Å^{-1} is rather similar to that for a-PS.[12]

Discussion

Kratky Function. As in the case of the previous SAXS measurements on a- and s-PMMAs,[6,7] the data for the Kratky function F_s in the range $k \lesssim 0.05$ Å^{-1} could not be obtained under the setting condition of the (point-focusing) SAXS camera for the present purpose. Thus we join the present data points to the previous ones[1] obtained for F_s in the range of small k by the use of the Kratky camera. Figure 4 shows plots of the data thus obtained for F_s against k for the four i-PMMA samples in acetonitrile at 28.0 °C. The unfilled, right-half-filled, left-half-filled, and top-half-filled circles represent the values for the samples iOM10, iOM31, iMM1, and iMMc10, respectively, the large and small circles representing the present and previous data, respectively. We note that measurements on the sample iMMc10 by the use of the Kratky camera had not been

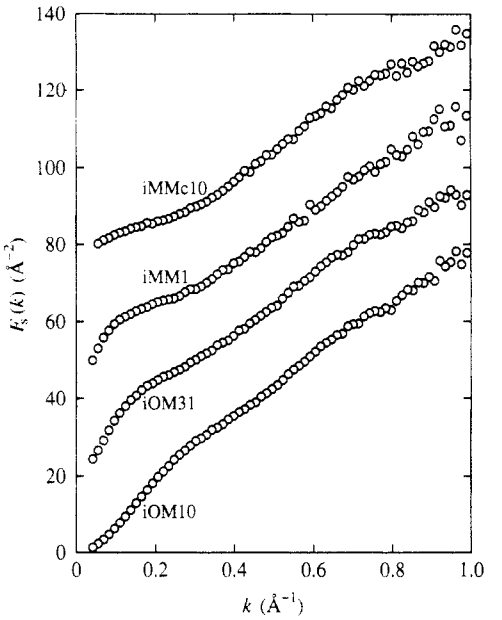

Figure 3. Plots of $F_s(k)$ against k for all the samples in acetonitrile at 28.0 °C, the data points for samples iOM31, iMM1, and iMMc10 being shifted upward by 20, 40, and 60 Å^{-2}, respectively.

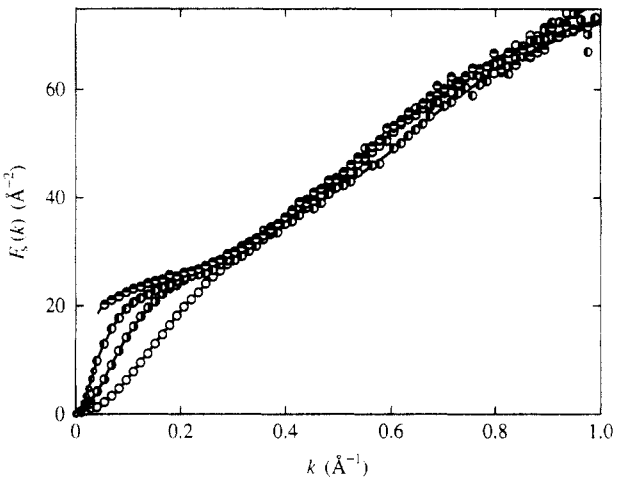

Figure 4. Plots of $F_s(k)$ against k for all the samples in acetonitrile at 28.0 °C: (○) iOM10; (◑) iOM31; (◐) iMM1; (◓) iMMc10. The large and small circles represent the present and previous[1] data, respectively. The solid curve connects the data points smoothly for each sample.

carried out in the previous study,[1] so that the plot does not contain the data points for that sample in the range of small k. It is seen that the present data points may be smoothly joined to the previous ones for the samples iOM10 through iMM1. This confirms the appropriateness and accuracy of the present determination of F_s described in the Results. Thus the solid curve connects the data points smoothly for each sample.

As mentioned in the Results, it is seen that F_s increases monotonically with increasing k for all the samples and does not exhibit the maximum and minimum as observed for a- and s-PMMAs with large M_w.[6,7] For the samples iOM31 through iMMc10, the slope of the tangent to each curve takes a minimum at $k \simeq 0.2$ Å^{-1}. It is also seen that the behavior of F_s is rather insensitive to the change in M_w in the range $k \gtrsim 0.4$ Å^{-1}, as in the case of a-PMMA.[6] This implies that the environment around the i-PMMA chain is independent of M_w, as in the case of a-PMMA.[6]

Comparison with the HW Theory. Now we make a comparison of the present and previous experimental data for F_s with the corresponding theory for the HW chain.

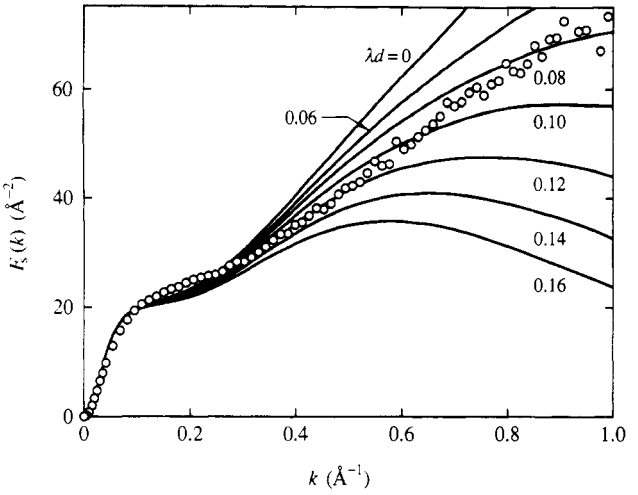

Figure 5. Comparison of the observed values of F_s for sample iMM1 with the HW theoretical values: (O) data in acetonitrile at 28.0 °C; (solid curves) HW theoretical values for the values of λd indicated.

The latter has been developed in a previous paper,[16] where the effect of chain thickness [i.e., thickness of the distribution of electrons (or hydrogen nuclei) around the HW chain contour] has been taken into account by adopting two simple models: the cylinder model and the touched-spheroid model. As in the case of the previous analysis of the SAXS data for a-PS[12] and a-PMMA,[6] we consider here only the former model, for simplicity.

For convenience, we reproduce here an outline of the numerical theoretical evaluation of the scattering function $P_s(k;L)$. For the HW cylinder model of total contour length L and diameter d, it is given by eq 25 with eqs 36–41 of ref 16 and may be written in the form

$$P_s(k;L) = 2L^{-2}\int_0^L (L-t)I(\mathbf{k};t)\,\{[F_0(kd)]^2 + g_2^{00}(t)[F_1(kd)]^2\}\,dt \quad (9)$$

where $I(\mathbf{k};t)$ is the characteristic function, i.e., the Fourier transform of the distribution function $G(\mathbf{R};t)$ of the end-to-end vector distance $\mathbf{R}$, for the HW chain of contour length t, F_n (n = 0, 1) are the functions given by eqs 40 and 41 of ref 16, which represent the effects of the (uniform) distribution of electrons (or hydrogen nuclei) within the (flexible) cylinder, and g_2^{00} is the angular correlation function[17] given by eq 38 of ref 16. The functions I and g_2^{00} are dependent also on the three basic model parameters of the HW chain, i.e., the constant differential-geometrical curvature κ_0 and torsion τ_0 of its characteristic helix taken at the minimum zero of its elastic energy and the static stiffness parameter λ^{-1}. We note that the function I may be evaluated numerically by the use of the weighting function and ϵ methods,[18] so that the integration over t in eq 9 must be carried out numerically. In order to compare the theoretical values of P_s as a function of k for given values of L and d with the experimental values, L may be converted to M_w by the use of the relation

$$L = M_w/M_L \quad (10)$$

with M_L the shift factor as defined as the molecular weight per unit contour length. The Kratky function F_s may then be calculated theoretically from eq 8 with eqs 9 and 10.

Figure 5 shows plots of F_s against k for the i-PMMA sample iMM1 in acetonitrile at 28.0 °C. The unfilled circles represent the (present and previous) experimental values, and the solid curves represent the corresponding

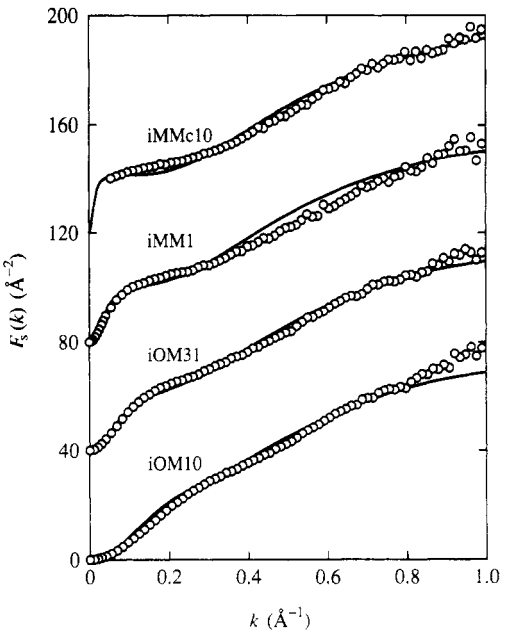

Figure 6. Comparison of the observed values of F_s with the HW theoretical values: (O) data in acetonitrile at 28.0 °C; (solid curves) best-fit HW theoretical values. The data points and theoretical curves for samples iOM31, iMM1, and iMMc10 are shifted upward by 40, 80, and 120 Å^{-2}, respectively.

HW theoretical values (for L = 329 Å) calculated from eq 8 with eqs 9 and 10 with the values of the model parameters determined from the previous analysis of $\langle S^2\rangle$,[1] i.e., $\lambda^{-1}\kappa_0$ = 2.5, $\lambda^{-1}\tau_0$ = 1.3, λ^{-1} = 38.0 Å, and M_L = 32.5 Å^{-1}, and with those of λd indicated. It is seen that, in the range $k \lesssim 0.1$ Å^{-1}, the theoretical values are insensitive to the change in λd and are in rather good agreement with the experimental ones. For larger k, however, the theory cannot give a quantitative explanation of the experimental results, although the disagreement between theory and experiment is not so large as in the case of a-PMMA.[6] Thus a theoretical curve such that, in the range of large k, its form is close to that of an experimental one as a whole is adopted as the "best-fit" theoretical curve, for convenience. In this case, the curve with λd = 0.08 is the best-fit one.

Figure 6 shows plots of F_s against k for all the i-PMMA samples in acetonitrile at 28.0 °C. The unfilled circles and the solid curves represent the (previous and present) experimental values and the "best-fit" HW theoretical values calculated from eq 8 with eqs 9 and 10 with the values of the model parameters mentioned above and with λd = 0.08, respectively. In the figure, the data points and the theoretical curves for the samples iOM31, iMM1, and iMMc10 have been shifted upward by 40, 80, and 120 Å^{-2}, respectively. It is seen that the theory may explain rather well the experimental data for all the samples except for the sample iMM1 over the whole range of k studied. However, this agreement between theory and experiment may be only accidental since there is no quantitative agreement for a-PMMA[6] in the range of large k. We note that the observed scattering function for a-PMMA there agrees nearly with that for i-PMMA, as shown later. Generally, the HW theory fails to reproduce quantitatively the behavior of the scattering function in the range of large k since it takes no account of the detailed distribution of scatterers. It is yet interesting to estimate the diameter d of the (excess) electron density distribution. We have d = 3.0 Å from the above values of λd and λ^{-1}, and the result is close to the value 2.8 Å evaluated previously for a-PMMA.[6] This agreement seems rather reasonable,

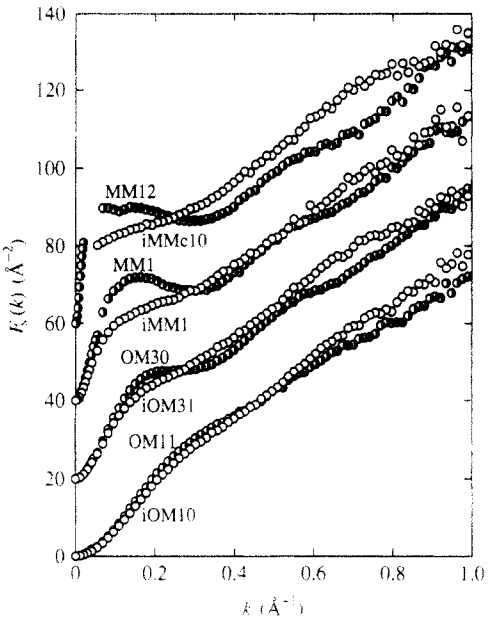

Figure 7. Comparison of the data for i-PMMA in acetonitrile at 28.0 °C with those for a-PMMA in acetonitrile at 44.0 °C: (○) i-PMMA; (◑) a-PMMA. The data points for samples iOM31 and OM30, those for iMM1 and MM1, and those for iMMc10 and MM12 are shifted upward by 20, 40, and 60 Å^{-2}, respectively.

considering the fact that the measurements for i- and a-PMMAs were carried out in the same solvent acetonitrile.

Comparison with the a- and s-PMMA Chains. We proceed to make a comparison of the present (and previous) SAXS data for F_s for i-PMMA with the previous ones for a-PMMA.[6] Figure 7 shows plots of F_s against k for all the i-PMMA samples indicated in acetonitrile at 28.0 °C (unfilled circles) and for the a-PMMA samples indicated in acetonitrile at 44.0 °C (right-half-filled circles). In the figure, the data points for the samples iOM31 and OM30, those for iMM1 and MM1, and those for iMMc10 and MM12 have been shifted upward by 20, 40, and 60 Å^{-2}, respectively. The values of M_w for the a-PMMA samples are 1.10×10^3, 2.95×10^3, 1.09×10^4, and 1.19×10^5 for the samples OM11, OM30, MM1, and MM12, respectively.[2,6] Thus, the i- and a-PMMA samples belonging to each pair have almost the same M_w, so that the figure may be considered to show the dependence on M_w of the difference between F_s's for i- and a-PMMAs with the same M_w.

For the pair with the lowest M_w, the data points for the two PMMAs exhibit almost the same behavior. This may be regarded as arising from the fact that the two PMMA chains take a rather similar global conformation for M_w sufficiently smaller than that value of M_w ($\simeq 5 \times 10^3$) at which the ratio $\langle S^2 \rangle / M_w$ for a-PMMA takes a maximum.[2] This is also consistent with the fact that the apparent mean-square radii of gyration $\langle S^2 \rangle_s$ for the two PMMAs are in rather good agreement with each other for small M_w (see Figure 5 of ref 1). For larger M_w, however, the data for the two PMMAs become different from each other in two ways as M_w is increased. First, in the range of small k, the data points for a-PMMA deviate appreciably upward from those for i-PMMA; F_s for the former exhibits the maximum and minimum for $M_w \gtrsim 10^4$, while it is a monotonically increasing function of k for the latter. Second, at $k \simeq 0.6$ Å^{-1}, the plot exhibits an inflection (or bump) for a-PMMA but not for i-PMMA, although the plots for them nearly agree with each other for all M_w in the range of large k ($\gtrsim 0.3$ Å^{-1}). These differences in the behavior of F_s may be regarded as arising from the

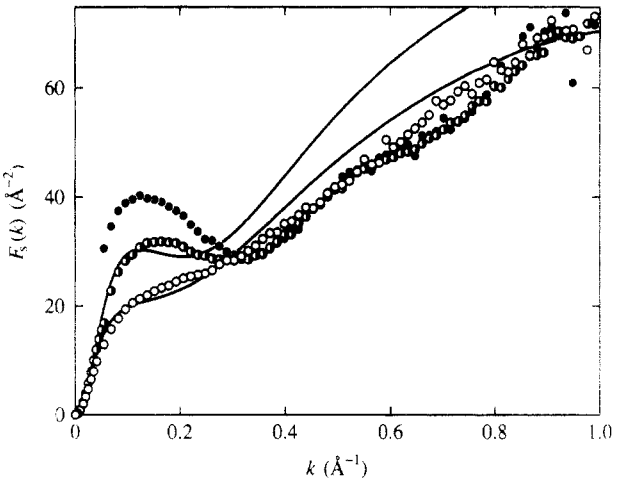

Figure 8. Comparison of the data for i-PMMA with those for a- and s-PMMAs: (○) present data for sample iMM1 in acetonitrile at 28.0 °C; (◑) previous data for an a-PMMA sample (MM1) with $M_w = 1.09 \times 10^4$ in acetonitrile at 44.0 °C;[6] (●) previous data for an s-PMMA sample with $M_w = 3.76 \times 10^4$ in acetonitrile at 44.0 °C;[7] (solid curves) best-fit HW theoretical values for i- and a-PMMAs.

difference in the local chain conformation between the two PMMAs with different f_r, as discussed in the previous paper,[1] i.e., from the fact that the i-PMMA chain is of weaker helical nature than the a-PMMA chain.

In order to make the dependence on f_r of the scattering profile more clear, we plot F_s for i-, a-, and s-PMMAs in Figure 8. In the figure, the unfilled and right-half-filled circles represent the same data for the i-PMMA sample iMM1 and a-PMMA sample MM1, respectively, as those presented in Figure 7, the filled circles represent the previous data for s-PMMA with $M_w = 3.76 \times 10^4$ in acetonitrile at 44.0 °C,[7] and the solid curves represent the best-fit HW theoretical values for i-PMMA (lower) and a-PMMA (upper). (For s-PMMA, we have not calculated the theoretical values because of the lack of values of the model parameters.) Note that the theoretical values for a-PMMA have been calculated from eq 8 with eqs 9 and 10 with the values of the HW model parameters, $\lambda^{-1}\kappa_0 = 4.0$, $\lambda^{-1}\tau_0 = 1.1$, $\lambda^{-1} = 47.0$ Å, and $M_L = 38.0$ Å^{-1}, and with the value 0.06 for λd.[6] It is clearly seen that, in the range $k \lesssim 0.3$ Å^{-1}, F_s becomes large as f_r is increased and that the oscillation appears for a-PMMA and more remarkably for s-PMMA, indicating that the latter chain is of much stronger helical nature than the former. We note that, although M_w of the s-PMMA sample is somewhat larger than those of the samples iMM1 and MM1, the theory[19] predicts that the increase in M_w in general causes only a shift of the maximum to the left but does not change the ratio of the maximum to the minimum. It is also interesting to see that, in contrast to the above remarkable difference between a- and s-PMMAs, the inflections of the plots at $k \simeq 0.6$ Å^{-1} for them are almost of the same degree. In sum, the HW theory may explain well the dependence of F_s on f_r, although only qualitatively in the range of large k.

Comparison with SANS Data. Finally, we make a comparison of the present SAXS data for F_s with small-angle neutron scattering (SANS) data. This is shown in Figure 9, where the unfilled circles represent the present SAXS data for the sample iMMc10 in acetonitrile at 28.0 °C and the filled circles represent the SANS data obtained by O'Reilly et al.[20] for an i-PMMA sample with $M_w = 1.20 \times 10^5$ and $f_r = 0.03$ in the bulk. For the latter data, we have adopted those corrected by Vacatello et al.[21] Although the value of M_w of the i-PMMA sample used by

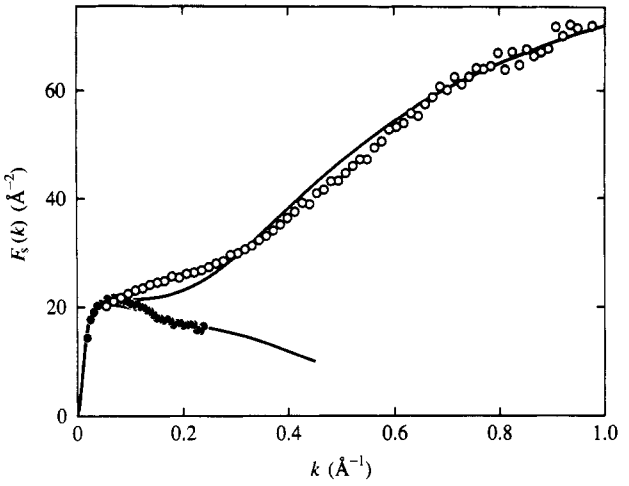

Figure 9. Comparison between SAXS and SANS data for i-PMMA: (○) present SAXS data for sample iMMc10 in acetonitrile at 28.0 °C; (●) SANS data for a sample with M_w = 1.20×10^5 by O'Reilly et al.;[20] (solid curves) respective best-fit HW theoretical values.

O'Reilly et al.[20] is somewhat larger than that of iMMc10, this difference in M_w is not so large as to have an appreciable effect on the profile of F_s (the Kratky plot), especially in the range of large k.

The two kinds of data agree with each other at $k \simeq 0.1$ Å^{-1}, while the SANS data deviate more and more downward from the SAXS data with increasing k. As discussed in the previous SAXS study of a-PMMA,[6] it is reasonable to attribute this disagreement between the two kinds of data in the range of large k to the difference in the distribution of scatterers between SAXS and SANS. For the former, the scatterers (electrons) may be considered to distribute in rather small regions around the α carbon atoms and the ester groups. On the other hand, for SANS, the scatterers are the hydrogen nuclei. Thus the effective thickness of the chain is smaller for SAXS than for SANS, so that F_s in the range of large k becomes larger for the former than for the latter.

In order to examine quantitatively the effect of the distribution of scatterers, we also compare the SANS data with the HW theory. The lower solid curve in Figure 9 represents the best-fit HW theoretical values with λd = 0.36 corresponding to the SANS data. (Note that the upper solid curve represents the HW theoretical values calculated above for the sample iMMc10.) We then obtain d = 13.7 Å. This value is remarkably larger than the value 3.0 Å evaluated from the SAXS data, as was expected, and it is rather consistent with the value 11.3 Å determined from the previous analysis[6] of the SANS data obtained by Dettenmaier et al.[22] for a-PMMA.

Conclusion

The scattering function P_s, or the Kratky function F_s, has been determined accurately for the unperturbed i-PMMA chains with various M_w, including the oligomers, each with the fraction of racemic diads $f_r \simeq 0.01$ in the range $k < 1$ Å^{-1}, by the use of a point-focusing SAXS camera in the High-Intensity X-ray Laboratory of Kyoto University. In contrast to the previous results for a- and s-PMMAs, for which F_s exhibits the maximum and minimum for large M_w in the range $k \lesssim 0.3$ Å^{-1}, it is always a monotonically increasing function of k for i-PMMA. On the other hand, F_s's for i-PMMA and a- (or s-) PMMA in the range $k \gtrsim 0.3$ Å^{-1} nearly agree with each other, although for the latter with large M_w it exhibits an inflection at $k \simeq 0.6$ Å^{-1}. The HW theory may explain well the experimental data for i-PMMA in the range not only of small k but also of large k. However, the agreement between theory and experiment in the range of large k may be only accidental. Important is the fact that the HW theory may give a good explanation of the difference in the behavior of F_s between i- and a-PMMAs on the basis of the values of the model parameters consistent with those determined from analyses of other dilute solution properties.

References and Notes

(1) Kamijo, M.; Sawatari, N.; Konishi, T.; Yoshizaki, T.; Yamakawa, H. *Macromolecules*, in press.
(2) Tamai, Y.; Konishi, T.; Einaga, Y.; Fujii, M.; Yamakawa, H. *Macromolecules* **1990**, *23*, 4067.
(3) Yamakawa, H. *Annu. Rev. Phys. Chem.* **1984**, *35*, 23.
(4) Yamakawa, H. In *Molecular Conformation and Dynamics of Macromolecules in Condensed Systems*; Nagasawa, M., Ed.; Elsevier: Amsterdam, 1988; p 21.
(5) Kratky, O.; Porod, G. *Recl. Trav. Chim. Pays-Bas* **1949**, *68*, 1106.
(6) Yoshizaki, T.; Hayashi, H.; Yamakawa, H. *Macromolecules* **1993**, *26*, 4037.
(7) Yoshizaki, T.; Hayashi, H.; Yamakawa, H. *Macromolecules* **1994**, *27*, 4259.
(8) Kirste, R. G.; Wunderlich, W. *Makromol. Chem.* **1964**, *73*, 240.
(9) Wunderlich, W.; Kirste, R. G. *Ber. Bunsen-Ges. Phys. Chem.* **1964**, *68*, 646.
(10) Ute, K.; Asada, T.; Miyatake, N.; Hatada, K. *Makromol. Chem., Macromol. Symp.* **1993**, *67*, 147.
(11) Sawatari, N.; Konishi, T.; Yoshizaki, T.; Yamakawa, H. *Macromolecules*, to be submitted for publication.
(12) Koyama, H.; Yoshizaki, T.; Einaga, Y.; Hayashi, H.; Yamakawa, H. *Macromolecules* **1991**, *24*, 932.
(13) Hayashi, H.; Hamada, F.; Suehiro, S.; Masaki, N.; Ogawa, T.; Miyaji, H. *J. Appl. Crystallogr.* **1988**, *21*, 330.
(14) Yamakawa, H. *Modern Theory of Polymer Solutions*; Harper & Row: New York, 1971; p 211.
(15) Berry, G. C. *J. Chem. Phys.* **1966**, *44*, 4550.
(16) Nagasaka, K.; Yoshizaki, T.; Shimada, J.; Yamakawa, H. *Macromolecules* **1991**, *24*, 924.
(17) Yamakawa, H.; Shimada, J. *J. Chem. Phys.* **1979**, *70*, 609.
(18) Yamakawa, H.; Shimada, J.; Fujii, M. *J. Chem. Phys.* **1978**, *68*, 2140.
(19) Yoshizaki, T.; Yamakawa, H. *Macromolecules* **1980**, *13*, 1518.
(20) O'Reilly, J. M.; Teegarden, D. M.; Wignall, G. D. *Macromolecules* **1985**, *18*, 2747.
(21) Vacatello, M.; Yoon, D. Y.; Flory, P. J. *Macromolecules* **1990**, *23*, 1993.
(22) Dettenmaier, A.; Maconnachie, A.; Higgins, J. S.; Kausch, H. H.; Nguyen, T. Q. *Macromolecules* **1986**, *19*, 773.